NASA Contractor Report 194882

ICASE Report No. 94-11

23 p

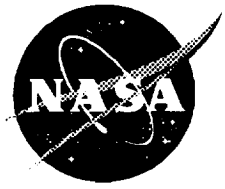

ICASE

A PREDICTOR-CORRECTOR SCHEME FOR VORTEX IDENTIFICATION

Bart A. Singer
David C. Banks

(NASA-CR-194882) A PREDICTOR-CORRECTOR SCHEME FOR VORTEX IDENTIFICATION Final Report (ICASE) 23 p

N94-33433

Unclas

G3/34 0009116

Contract NAS1-19480
March 1994

Institute for Computer Applications in Science and Engineering
NASA Langley Research Center
Hampton, VA 23681-0001

Operated by Universities Space Research Association

A Predictor-Corrector Scheme For Vortex Identification

Bart A. Singer *

High Technology Corporation
Mail Stop 156, NASA Langley Research Center
Hampton, VA 23681

David C. Banks **

Institute for Computer Applications in Science and Engineering
Mail Stop 132C, NASA Langley Research Center
Hampton, VA 23681

ABSTRACT

A new algorithm for identifying and characterizing vortices in complex flows is presented. The scheme uses both the vorticity and pressure fields. A skeleton line along the center of a vortex is produced by a two-step predictor-corrector scheme. The technique uses the vector field to move in the direction of the skeleton line and the scalar field to correct the location in the plane perpendicular to the skeleton line. A general vortex cross section can be concisely defined with five parameters at each point along the skeleton line. The details of the method and examples of its use are discussed.

---

* This author was supported by the Theoretical Flow Physics Branch at NASA Langley Research Center under contract NAS1-19299.

** This author was supported by the National Aeronautics and Space Administration under NASA contract No.NAS1-19480 while the author was in residence at the Institute for Computer Applications in Science and Engineering (ICASE), NASA Langley Research Center, Hampton, VA 23681.

1 Introduction

Vortices are considered the most important structures that control the dynamics of flow fields. Large-scale vortices observed in atmospheric and oceanographic flows are responsible for ozone holes, hurricanes, tornadoes, and maelstroms. Vortices that are shed from aircraft canards, wings, and control surfaces affect the handling characteristics of the airplane and determine the closest safe following distance of other aircraft. On a smaller scale, vortices are the fundamental building blocks of turbulent flow structures and are intimately connected with the mixing of chemical species, heat transfer, and drag forces.

Although the term "vortex" connotes a similar concept in the minds of most fluid dynamicists, a precise definition is difficult to obtain. Robinson [1] suggests the following working definition: "A vortex exists when instantaneous streamlines mapped onto a plane normal to the vortex core exhibit a roughly circular or spiral pattern, when viewed from a reference frame moving with the center of the vortex core." Unfortunately, this definition requires a knowledge of the vortex core before one can determine whether something is a vortex. In practice, Robinson [2] and Robinson, Kline, and Spalart [3] use the above rigorous definition to confirm that a particular structure is, in fact, a vortex. Regions of low pressure are used to identify candidate vortices. Their scheme exploits the fact that the pressure in the core of a vortex is lower than that of the surrounding fluid. A radial force is needed to provide the centripetal acceleration that keeps a particle rotating about an axis. In the case of vortices, this force is in the form of the pressure; the pressure inside a vortex is lower than the pressure outside the vortex. Robinson and his colleagues find that elongated low-pressure regions in incompressible turbulent flows almost always indicate vortex cores, but these surfaces can be difficult to characterize and provide no information in regard to the sense of rotation or the connectivity between the structures.

Moin and Kim [4] and Kim and Moin [5] use vorticity lines (sometimes called vorticity field lines or vortex lines) to visualize vortical structures in turbulent channel flow. A vorticity line is everywhere parallel to the local vorticity vector and is defined by

$$\frac{d\vec{x}}{ds} = \frac{\vec{\omega}}{|\vec{\omega}|} \tag{1}$$

where $\vec{\omega} = \nabla \times \vec{u}$ is the vorticity vector, $\vec{u}$ is the velocity vector, $\vec{x}$ is the location in space, and s is the distance along the vorticity line. The definition suggests that vorticity lines should go through the cores of vortices, which is usually the case. However, the resulting vortex lines are extremely sensitive to the choice of initial location for the integration. As Moin and Kim [4] point out, "If we choose $\vec{x}_0$ arbitrarily, the resulting vortex line is likely to wander over the whole flow field like a badly tangled fishing line, and it would be very difficult to

identify the organized structures (if any) through which the line may have passed." Kim and Moin [5] illustrate the potential tangle in their Fig. 2. To avoid such a confusing jumble, they carefully select the initial points (inside suspected vortices) and focus on specific parts of the resultant lines to illustrate some important features of turbulent channel flow. However, Robinson [1] shows that even experienced researchers can be surprisingly misled by ordinary vorticity lines.

Villasenor and Vincent [6] present an algorithm for the recognition and visualization of elongated vortices in three-dimensional time-dependent flow fields. They start from a seed point and compute the average length of all vorticity vectors contained in a small-radius cylinder. The axis of the cylinder extends from the seed point to the surface of a sphere centered about the seed point. They repeat this step for a large number of cylinders that emanate from the seed point. The cylinder with the maximum average vorticity vector length becomes a segment of the vortex tube. This process is repeated until the vorticity decreases enough to end the vortex tube. Because the scheme depends only on the magnitude of the vorticity vectors rather than their direction, the algorithm must limit the angle between adjacent line segments so that the new line segment is different from the previous line segment traced in the opposite direction. All vorticity vectors inside the vortex tube are drawn. The process can be repeated for multiple time steps so that the evolution of the vortex tubes is visualized as a sequence of all stored vorticity vectors. Villasenor and Vincent [6] claim that the use of only the magnitudes and not the directions of the vorticity vectors is advantageous because it allows the algorithm to find structures that do not have axes aligned with the principal axis of the structure. As a consequence, the algorithm can inadvertently capture structures that are not vortices. In addition, by visualizing all vectors that are inside the cylinder, structures are included that are not part of the vortex originally intended to be viewed. An example can be seen in Fig. 4(c) of Villasenor and Vincent [6], in which another structure is responsible for some of the vorticity vectors that are almost orthogonal to the vortex axis.

Zabusky, Boratav, Pelz, Gao, Silver, and Cooper [7] fit ellipsoids to surfaces of constant vorticity $|\vec{\omega}|$ and to constant vortex stretching $|\vec{\omega} \cdot \nabla \vec{u}|/|\vec{\omega}|$ in an effort to understand the dynamics of a vortex reconnection process. A bundle of vector field lines of the vorticity $\vec{\omega}$ and the vortex stretching $\vec{\omega} \cdot \nabla \vec{u}$ emanate from the major and minor axes and from the center of the minor ellipse of the respective fitted ellipsoids. Both the ellipsoids and the vector field lines provide useful information about the vortices for their flow field, which contains neither solid boundaries nor a mean straining field. In flows with these additional complications, the regions with large vorticity magnitudes do not necessarily correspond to vortices; hence, ellipsoids of constant vorticity coupled with vorticity lines are unlikely to

provide useful characterizations.

Chong, Perry, and Cantwell [8] address the question of when a region of vorticity is a vortex. They suggest that a vortex core is a region where the velocity-gradient tensor has complex eigenvalues. In such a region, the rotation tensor dominates over the rate-of-strain tensor. Soria and Cantwell [9] use this approach to study vortical structures in free-shear flows. At those points at which the vorticity magnitude exceeds a specified fraction of the maximum vorticity, the eigenvalues of the velocity-gradient matrix are determined. Those regions that have complex eigenvalues and satisfy the vorticity-threshold criterion are rendered as solid surfaces that represent the vortices in the flow. This method correctly identifies the large vortical structures in the flow. However, the method clutters the picture with many smaller structures and does not provide a way to link the smaller vortical volumes with the larger coherent vortices of which they might be a part.

Yates and Chapman [10] carefully explore two definitions of vortex cores. One definition associates a vortex core with a streamline of minimum curvature within a region of spiraling streamlines. The other definition regards the vortex core as the line defined by the local maxima of normalized helicity. Under certain circumstances, both definitions produce the same vortex core. Unfortunately, all of the analyses and conclusions are appropriate only for steady flows.

Bernard, Thomas, and Handler [11] use a semiautomated procedure to identify quasi-streamwise vortices in the near-wall region of turbulent-channel-flow direct-numerical-simulation data. Their method finds local centers of rotation in user-specified regions in planes perpendicular to the streamwise direction. The local centers of rotation are linked to corresponding centers in adjacent streamwise-normal planes to form a vortex-core line. The results of their work indicate that experienced users can correctly find essentially all critical vortices responsible for the maintenance of the Reynolds stress. However, their method fails to capture vortices with axes that are not nearly aligned with the streamwise direction. This shortcoming can be a major difficulty for flows such as free-shear layers and transitional boundary layers, in which both streamwise- and spanwise-oriented vortices are important. In addition, the procedure depends heavily on user intervention to indicate regions where the program should search for centers of rotation. This process is tedious, and the detailed results depend upon nonquantifiable whims of the user.

Here, we present a new approach for identifying and characterizing vortices in complex flow fields. Rather than a dependence upon a single quantity to define the vortex, the new approach is a predictor-corrector method that converges to the vortex skeletons (the lines that pass through the vortex cores). In section 2, we describe how the new method determines the vortex skeletons. In section 3, we discuss some novel vortex cross-section

schemes that put meat on the skeleton lines, and we summarize our findings in section 4.

2 The vorticity-predictor pressure-corrector method

Our new predictor-corrector method produces an ordered set of points that approximates the skeleton of a vortex. Associated with each point are quantities that describe the local characteristics of the vortex. These quantities may include the vorticity, the pressure, cross-sectional information, the circulation, and other quantities of interest.

The new method produces lines that are similar to vorticity lines. However, because a distinction exists between the vorticity, which is a mathematical function of the instantaneous velocity field, and a vortex, which is a physical structure with coherence over a region of space, the straightforward integration of the vorticity lines must be modified to locate the skeleton lines associated with individual vortices. At the very least, because vorticity lines can begin and end only at domain boundaries and vortices have no such restriction, we must develop criteria for initiating and terminating the integration. In addition, the method must be self-correcting (i.e., line trajectories that diverge from the vortex core should be subject to a restoring (correcting) force).

In this section, we will first discuss the procedure used to find an initial point on the vortex-core skeleton. Then we will reveal the details involved in growing the vortex-core skeleton from the seed point. Finally, the termination of the vortex skeleton will be addressed.

2.1 Finding a seed point

Any flow-field information can be used to find starting locations for the predictor-corrector process. The pressure and the vorticity magnitude are convenient scalars for choosing seed points. In our work, the flow field is scanned in planes perpendicular to the streamwise direction. The scanning direction affects the order in which vortices are located, but not the overall features of the vortices. In each plane, the values of the pressure and the vorticity magnitude are checked. Threshold values can be chosen a priori, or they can be a predetermined fraction of the extrema. If the pressure is less than the pressure threshold and the vorticity magnitude is greater than its threshold, then the point location is further refined. In our implementation, this positional refinement shifts the seed point to the location of the local pressure minimum in the plane perpendicular to the vorticity vector. (The rationale for this refinement will be discussed later.) The sampling can be done at every grid point. We experimented with sampling at every second, third, and fourth points. Although a test of each grid point to determine if the specified pressure and vorticity criteria are met is not expensive, we had hoped that sampling for seed points on a coarser mesh would eliminate

the multitude of redundant vortices that we found. Global coarsening of the grid does not uniformly eliminate the problem; some of the redundancies are avoided, but others remain.

A better method for eliminating the redundant vortices involves the selective elimination of grid points from the supply of possible seeds. Elements of a three-dimensional integer array correspond to volumes about each grid point. All of the elements are originally set to zero. For the first vortex, any point in the flow field may be evaluated as a potential seed point. As points are added to the vortex skeleton, the elements of the integer array associated with the points are flagged. The flagged points will not be available as seeds for subsequent vortices. Although many coincident vortices are eliminated in this way, a further reduction can be achieved by also flagging elements of the array that correspond to points that are within the vortex cross section. In Fig. 1, multiple skeleton lines started from different seed points all pass through the same vortex tube. The redundancies are eliminated when points inside a tube are excluded from the pool of future seed points.

2.2 Growing the skeleton

Once a seed point has been selected, the skeleton of the vortex core can be grown from this point. The scheme that we have developed is a two-stage predictor-corrector method. With this technique, the next position of the vortex skeleton is predicted by integrating along the vorticity vector. This candidate location is corrected by adjusting the position to the pressure minimum in the plane that is perpendicular to the vorticity vector. To ensure that the minimum is actually part of the vortex under consideration, only a limited angle between the vorticity vectors at the predicted and the corrected point is allowed. [1] The continuous modification of the vorticity-line location lessens the sensitivity to both the initial conditions and the integration details. These sensitivities are common problems in vorticity-line calculations. Just as importantly, the corrector stage decreases the influence of background mean shear and small-scale vorticity fluctuations on the identification of the vortex cores. The identified vortex skeleton corresponds more closely to what one might intuitively choose as the vortex skeleton than to the standard vorticity-line result.

The modified vortex-line scheme is illustrated in the schematic diagrams of Fig. 2 and is also summarized in pseudocode below.

[1] This differs from the angle limitation imposed by Villasenor and Vincent [6]. They restrict the change in direction of the skeleton line along the center of the vortex tube from one point on the skeleton line to the next. We restrict the change in the direction of the vorticity vector from the predicted location to the corrected location.

For each remaining seed point

If the seed point p_0 is not in any previous vortex

While the vortex skeleton continues

1. Determine vorticity $\vec{\omega}_i$ at p_i
2. Integrate vorticity to find $\tilde{p}_{i+1}$ (predictor)
3. Determine vorticity $\tilde{\vec{\omega}}_{i+1}$ at $\tilde{p}_{i+1}$ (corrector)
4. Find location p_{i+1} of minimum pressure in plane perpendicular to $\tilde{\vec{\omega}}_{i+1}$ at $\tilde{p}_{i+1}$
5. Calculate quantities of interest at p_{i+1}
6. $i \leftarrow i + 1$

The calculation of the vortex skeleton proceeds both forward and backward from the seed point. The details for continuing the calculation from one point to the next are indicated by the numbered items in the pseudocode. Processes 1 and 2, which are shown in Fig. 2(a), represent the predictor stage of the algorithm. The corrector stage is summarized by processes 3 and 4, which are illustrated in Figs. 2(b) and 2(c). We iterate the corrector stage so that the pressure at position p_{i+1} is the local minimum in the plane perpendicular to $\vec{\omega}_{i+1}$. We restrict the movement in the corrector steps by limiting the angle between $\vec{\omega}_{i+1}$ and $\tilde{\vec{\omega}}_{i+1}$. The resultant state, which is illustrated in Fig. 2(d), is equivalent to that in Fig. 2(a), except that the index $i + 1$ replaces the index i.

The effectiveness of the predictor-corrector scheme is illustrated in Fig. 3, in which data from the direct numerical simulations of Singer and Joslin [12] are analyzed. The transparent vortex tube is constructed with data from the full predictor-corrector method. Its core is indicated by the darker skeleton. The lighter skeleton follows the uncorrected integral curve of the vorticity. It is obtained by disabling the corrector phase of the scheme. The vorticity line deviates from the core, exits the vortex tube entirely, and wanders in the flow field.

Although the general behavior of the predictor-corrector algorithm is reliable and robust, optimal performance of the technique requires careful attention to implementation details. The remainder of this subsection addresses issues that are important to the successful use of this method.

2.2.1 Eliminating feeder vortices

Because the vorticity near the edge of a vortex may be skewed with respect to the vorticity at the vortex center, the location of the pressure minimum in the plane perpendicular to the edge vorticity might not be in the vortex center. This potential mismatch of the pressure-minimum

and the vortex-center locations is rarely a problem in the vortex skeleton-line calculations because the predictor-corrector method inhibits large excursions from the vortex center. However, a seed point might be selected near the vortex edge. In this case, adjustment of the point location to the pressure minimum might still result in a point that is far from the vortex center. These situations result in small "feeder vortices" that spiral toward the vortex center. Examples of feeder vortices are illustrated in Fig. 4. We found that we can eliminate most of these feeder vortices by taking advantage of the asymmetry of the predictor-corrector method. In either forward or backward mode, the predictor-corrector scheme will converge to a vortex center. We can eliminate the feeder vortices by redefining the initial point (i.e., the point at which we start recording the elements on the skeleton line) to be the location after a fixed number (usually 5 to 10) of predictor-corrector steps. If the original seed point is located on the vortex core, the method will return to the seed on the backward integration path. However, if the original seed point is located on a feeder vortex, then the backward integration will miss the original seed point and the skeleton of the feeder vortex. Instead, the retraced skeleton line will closely follow the vortex center. Although the use of many integration points before the initial point will eliminate feeder vortices, this practice will also limit the minimum extent of any detected vortices.

2.2.2 Numerical considerations

Neither the pressure minimum nor the result of the vorticity-line integration is likely to be on a grid point; hence, we must choose an interpolation scheme to find the pressure and vorticity at arbitrary locations in the flow field. Our first experiments with trilinear interpolation were a disappointment. No local extrema could be found between two points connected by a straight line. To allow the local pressure minima to exist in the interior of a grid cell, a higher order interpolation method is necessary. Second-order interpolation would use three grid points: two from one side of the desired location and one from the other side. To reduce any bias from the interpolation, a four-point Lagrange interpolation is used in each of the three coordinate directions. When the outer points of the four-point method are not in the domain, two-point Lagrange (linear) interpolation is used. The complete interpolation scheme works quite well, although it requires more computer time than any other subroutine in the computer program.

The vorticity integration can be performed with a variety of methods. First, we used a fourth-order Runge-Kutta approach. This produced satisfactory results; however, step-size optimization was difficult to automate. Instead, we developed a new technique whereby the point-to-point distance in the vorticity integration is always equal to the smallest dimension of the local grid cell. The new point location is found by advancing this distance in the

direction of the local vorticity vector. This procedure ensures that successive points will not be more than one grid cell apart, so that if the original calculation is well resolved, then the vorticity-line calculation will also be sufficiently resolved. The procedure also reduces the chance of wasting many calculations inside a single grid cell.

2.2.3 Pressure-minimum corrector step

The pressure-minimum correction scheme uses the method of steepest descent to find the local pressure minimum in the plane perpendicular to the vorticity vector. First, the vorticity vector at the candidate point is determined by interpolation from the surrounding grid points. Two perpendicular unit vectors $\hat{f}$ and $\hat{g}$ (Fig. 5) are determined in the plane normal to the vorticity vector. The smallest grid-cell dimension d is used as a local length scale to find two points in the plane in the $\hat{f}$ and $\hat{g}$ directions. The pressures at these two points and the current point are used to form the in-plane pressure-gradient vector. A sample point is chosen at a distance d from the current point in the direction opposite to the pressure-gradient vector. If the pressure at the new sample point is less than the pressure at the current point and the dot product of the vorticities at the sample and current points is greater than a specified value (0.90–0.95 works well), then the new sample point becomes the current location and the process is repeated. If the sample point has a greater pressure than the current point, then the distance d is halved and a new sample-point comparison is made. If the orginal point is still the point of minimum pressure after d has been halved twice, then one last check for a possible minimum is made in the direction of the positive gradient. (Rare circumstances with a great deal of symmetry can produce a pressure-gradient vector that is in the wrong direction.) Failure to find any points with lower pressure leads to acceptance of the current point as the next point on the vortex-core skeleton.

2.3 The end of the line

Vorticity lines extend until they intersect a domain boundary, but vortices typically begin and end inside the domain. Here, we discuss some techniques for stopping the integration. One particularly clean termination occurs when the vortex cross section, which will be discussed in the next section, has zero area. This approach provides smooth surfaces for visualization with no abrupt vortex-tube cutoffs in the direction that is tangential to the vorticity. Although we have used this line-termination technique successfully, the method can fail to show connections between parts of the same vortex. For instance, if a low-intensity region exists between high-intensity regions of the same vortex, then the low-intensity region might not satisfy the criteria for a finite cross section. If both high-intensity regions have

finite cross sections, then the single vortex can be educed as two small disconnected vortices. Although the criteria that define the lateral edge of the vortex can be weakened to ensure that the low-intensity region has a finite cross section, the problem can potentially reemerge with a new vortex that is educed with the weaker cross-section criteria. Our resolution of this problem exploits the asymmetric nature of the predictor-correction method.

Because the predictor-corrector method will follow the core of a vortex regardless of the criteria used to define the vortex cross section, the vortex skeleton line is continued even when the cross-sectional area of the vortex is equal to zero. The vortex of interest can either reintensify or dissipate. If the vortex reintensifies, then the continuation of the vortex skeleton line will provide a link between the two more intense regions of the vortex. This link can be visualized as a thread that connects the two disjoint regions, or the two regions can simply be rendered with the same color or texture. On the other hand, if the vortex dissipates, then the vortex skeleton line continuation will wander through the flow field and eventually either intercept a domain boundary or enter a new vortex. If a domain boundary is reached, then the elements of the vortex skeleton line that were computed after the cross-sectional area became zero are discarded. These same points are also discarded if the vortex skeleton line enters a new vortex with a nonzero cross-sectional area. To determine whether the new region of finite cross section is a continuation of the original vortex or an entirely new vortex, we march the predictor-corrector scheme backwards for the same number of steps taken since the previous region of nonzero cross section was exited. Some possible scenarios are illustrated in Fig. 6. In Fig. 6(a), the skeleton line leaves the first vortex tube at point P_1 and continues for N steps until it encounters the second vortex tube at point P_2. The predictor-corrector scheme is then marched backwards N steps from P_2 to P_3. The distance between points P_1 and P_3 is small relative to the distance between P_1 and P_2 (a 10-percent criterion is used); hence, the link between P_1 and P_2 is most probably a low-intensity vortex, and we keep the thread between these vortex tubes. However, in Fig. 6(b) the vortex tube that ends at P_4 continues to dissipate, and the continuation of its skeleton line lacks clear direction and wanders through the flow field. The line intercepts another vortex tube at P_5 after M steps. The predictor-corrector method is marched backwards M steps from P_5 to P_6. Initially, the reverse integration retraces the forward integration, but halfway between P_5 and P_6 the two lines diverge rapidly and become uncorrelated. The distance from P_4 to P_6 is a large fraction of the distance from P_4 to P_5, so the algorithm concludes that the vortex tube intersected at P_5 is different from the vortex tube that ends at P_4. The points on the vortex skeleton line that connect the two tubes are discarded, and the vortex skeleton is terminated. Finally, in Fig. 6(c), the continuation of the skeleton line of the vortex tube that ends at point P_7 intersects the side of another vortex tube (shown as a wireframe) and

is immediately taken to the pressure minimum at P_8. The reverse integration for this case is along the axis of the new vortex tube away from the original vortex. The point P_9 is far from P_7; hence, the two vortex tubes are distinct from each other and the line connecting them is discarded.

3 Putting meat on the bones

The determination of an appropriate vortex cross section has been one of the more difficult practical aspects of this work. For isolated vortices, a simple pressure criterion to define the edge of a vortex works quite well, although the information content of the visualization is little more than that which is available from pressure isosurfaces. In regions where vortices interact, the pressure alone is inadequate. The low-pressure regions from two or more vortices can merge and distort the radius estimate of any single vortex. A similar problem arises if the vortex edge is defined in terms of vorticity magnitude. This particular difficulty is resolved if the angle between the vorticity vector on the skeleton line and the vorticity vector at any radial position is restricted. Any angle greater than 90° indicates that the fluid at the radial position is rotating in the direction opposite to that in the core. The vortex circulation Γ is defined as

$$\Gamma = \oiint_S \vec{\omega} \cdot \hat{\vec{n}} dA \tag{2}$$

where $\hat{\vec{n}}$ is a unit vector normal to the surface S; dA is an area element on the surface S; and S is a cross-sectional surface of the vortex. The vortex circulation increases as the cross-sectional area increases, provided that the angle between the vorticity vector at a given radial position and the vorticity vector on the skeleton line is less than 90°. This observation suggests the use of the 90° variation in vorticity vectors as a single vortex-edge criterion. Unfortunately, in a uniform shear flow, this criterion results in an infinite cross section because the vorticity at all radial locations is the same. In practice, we have found that the 90° restriction works well in combination with a low-pressure criterion for the vortex edge. For the actual computation of the radial distance, the pressure and the vorticity must be sampled along a number of radial lines perpendicular to the vortex skeleton line. We sample at an increment that is equal to the minimum grid-cell dimension at the skeleton line. The dot product of the vorticity at the radial point with the vorticity on the skeleton line must be greater than zero for the 90°-variation criterion to hold. At each position, this dot product and the pressure are checked to ensure that they both satisfy the respective requirements. If either fails, the radial position along that line is the point of failure as determined by linear interpolation between the two most recent sample points. By sampling along radial lines that emanate from a point on the skeleton line, we implicitly require that the cross section

be starlike (i.e., each radial line will intersect the cross-section boundary only once.) Cross sections with more complicated geometries are truncated to a starlike form.

Relative measures for the vortex edge are also possible. A relative measure defines the vortex edge as the position at which some quantity decreases below a specified fraction of its value on the skeleton line. Clearly, this measure will always give a finite cross section, and the cross section can become infinite in a uniform shear flow. We have found that relative measures are not as informative as the absolute measures.

The characterization of the cross section can take many forms. The detailed aspects of the data are most nearly recovered if the radial location of the vortex edge is retained at many closely spaced azimuthal angles. If the radius of the cross section were sampled at 10° increments in the azimuthal direction, then 36 radial distances and a reference vector at every position along the vortex skeleton line would need to be stored. For the minimal-storage approach that provides characteristic cross-sectional information, all of the radial distances are averaged to obtain a single scalar radius. No reference vector is needed if only the radius is used, so this simple method uses the least amount of storage. We have found that the radius is a very good cross-section descriptor for isolated vortices. When vortices begin to interact, the radius does not provide a good description of the asymmetric distortion experienced by the vortices. However, the first few coefficients of the Fourier series of the radial locations provides a convenient compromise between the simple radius approach and a full description of all radial locations. The series are easy to compute, easy to interpret, and allow a large range of cross-sectional shapes. In our work, we keep the constant term (which is the radius), the first and second sine and cosine coefficients, and a reference vector. Most of the cases that we have checked have a factor-of-10 drop in the magnitude of the first and second coefficients, a fact that suggests that the series is convergent. Figure 7 illustrates a single cross section of a vortex educed from direct numerical simulation data. The shaded region represents the interior of the vortex tube, the boundary of which was determined by sampling along lines that radiate from the cross (which marks the skeleton-line location) at 1° intervals. The dashed line is a circle centered about the skeleton-line location with the averaged radius of the vortex tube. The solid line is the two-term Fourier series representation of the vortex cross section. Note how the vortex boundary represented by the Fourier series more nearly shows both the eccentricity and the flattening of the vortex tube compared to the circular cross section.

ORIGINAL PAGE IS
OF POOR QUALITY

4 Conclusions

The innovative use of a two-step predictor-corrector algorithm has been introduced to educe vortices from flow-field data. Rather than relying on any single quantity to determine the vortex skeleton line, the new method uses vorticity to predict the new location of the next element along the line and then corrects this location by using the pressure field in the plane perpendicular to the vorticity vector. The prediction stage resembles a portion of a vorticity-line calculation; the correction stage maintains the line near the vortex center. Unlike other approaches, our method is able to treat the skeleton line through the vortex core as an attractor in the flow field.

To make the method work in all but the simplest flow fields, numerous side issues, which are common to all techniques that grow a skeleton line from seed points, must be addressed. This paper discusses a number of novel approaches that we have developed to deal with matters such as seed-point selection, feeder-vortex elimination, vortex skeleton-line termination, and vortex cross-section description. Sample extractions of vortices from various flow fields illustrate the different aspects of the technique.

The predictor-corrector technique presented here can identify vortices in flow fields that are far more complex than those that we have used here for illustration purposes. An extension of the direct numerical simulation of Singer and Joslin [12] provides one of the more interesting flow configurations that we have considered. The predictor-corrector algorithm educes a complex tangle of many interconnected vortices that are visualized in Fig. 8. All of the implementation features discussed above are used to identify the vortices in this messy flow field.

Although many modifications can be made to the basic scheme, the principle of using a vector field to predict the location of the next point and a scalar field to correct this position distinguishes this method from others.

References

[1] S. K. Robinson, "Coherent motions in the turbulent boundary layer," *Annu. Rev. Fluid Mech.* **23**, 601 (1991).

[2] S. K. Robinson, "A review of vortex structures and associated coherent motions in turbulent boundary layers," in *Proceedings of Second IUTAM Symposium on Structure of Turbulence and Drag Reduction*, Federal Institute of Technology, Zurich, Switzerland, July 25-28 (1989).

[3] S. K. Robinson, S. J. Kline, and P. R. Spalart, "A review of quasi-coherent structures in a numerically simulated boundary layer," NASA TM-102191 (1989).

[4] P. Moin, and J. Kim, "The structure of the vorticity field in turbulent channel flow. Part 1. Analysis of instantaneous fields and statistical correlations," *J. Fluid Mech.* **155**, 441 (1985).

[5] J. Kim, and P. Moin, "The structure of the vorticity field in turbulent channel flow. Part 2. Study of ensemble-averaged fields," *J. Fluid Mech.* **162**, 339 (1986).

[6] J. Villasenor and A. Vincent, "An algorithm for space recognition and time tracking of vorticity tubes in turbulence," *CVGIP: Image Understanding* **55**:1, 27 (1992).

[7] N. J. Zabusky, O. N. Boratav, R. B. Pelz, M. Gao, D. Silver, and S. P. Cooper, "Emergence of coherent patterns of vortex stretching during reconnection: A scattering paradigm," *Phys. Rev. Let.* **67**:18, 2469 (1991).

[8] M. S. Chong, A. E. Perry, and B. J. Cantwell, "A general classification of three-dimensional flow fields," *Phys. of Fluids A* **2**:5, 765 (1990).

[9] J. Soria, and B. J. Cantwell, "Identification and classification of topological structures in free shear flows," in *Proceedings of IUTAM Eddy Structure Identification in Free Turbulent Shear Flows* (1992).

[10] L. A. Yates, and G. T. Chapman, "Streamlines, Vorticity Lines, and Vortices," AIAA Paper 91-0731 (1991).

[11] P. S. Bernard, J. M. Thomas, and R. A. Handler, "Vortex dynamics and the production of Reynolds stress," *J. Fluid Mech.* **253**, 385 (1993).

[12] B. A. Singer, and R. D. Joslin, "Metamorphosis of hairpin vortex into a young turbulent spot," submitted to *Phys. Fluids A* (1993).

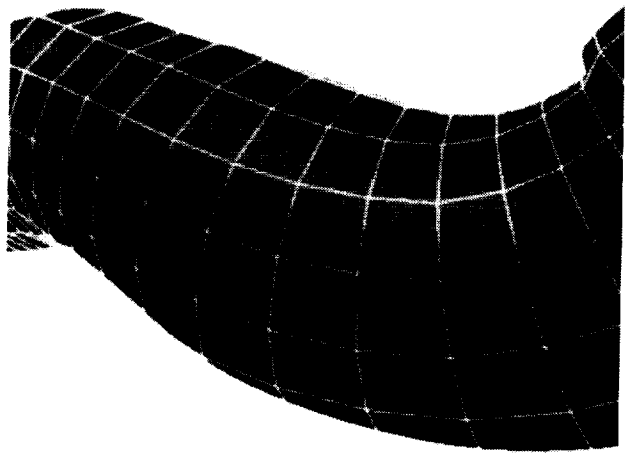

Figure 1: Multiple realizations of same vortex tube from different seed points.

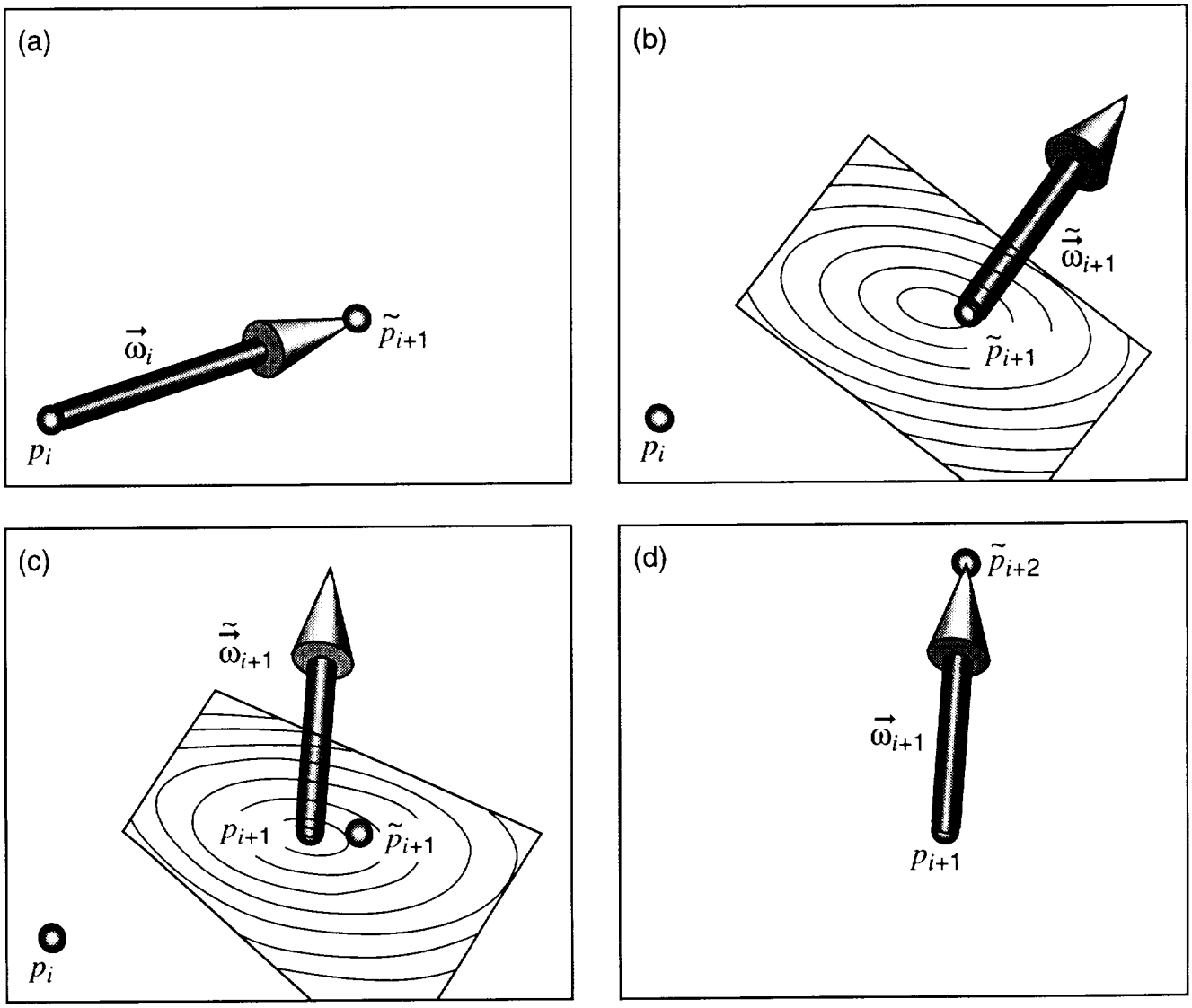

Figure 2: Schematic of predictor-corrector algorithm. (a) Vorticity $\vec{\omega}_i$ is used to predict candidate point $\tilde{p}_{i+1}$. (b) Pressure is determined in plane perpendicular to vorticity $\tilde{\vec{\omega}}_{i+1}$. (c) New point on skeleton line p_{i+1} is corrected to pressure minimum in plane perpendicular to vorticity $\tilde{\vec{\omega}}_{i+1}$. (d) Repeat at point p_{i+1}.

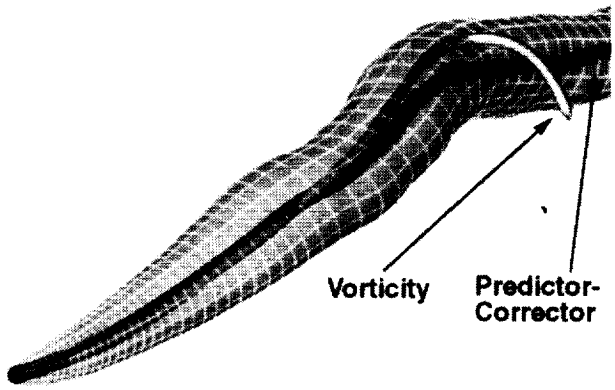

Figure 3: Standard vorticity lines are compared with results from predictor-corrector scheme. Both results use same flow data and same computer code. Standard vorticity lines are obtained by disabling corrector portion of program. Transparent tube is constructed from data from predictor-corrector method.

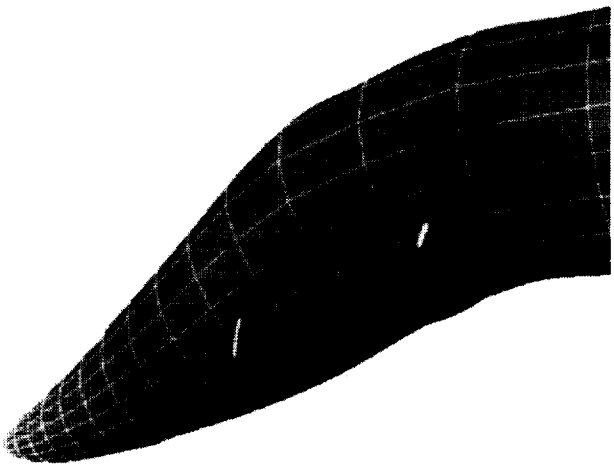

Figure 4: Feeder vortices merge with a large-scale hairpin vortex. Points that satisfy seed-point criteria exist on edge of vortex tube. They curve inward toward centerline and then follow main skeleton line.

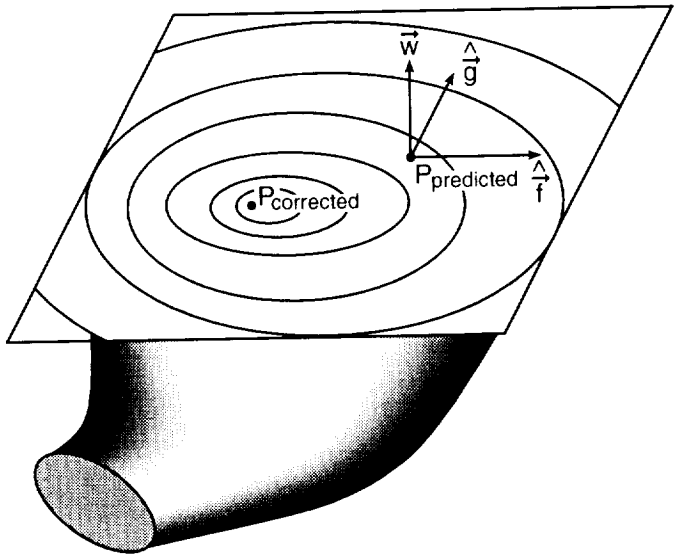

Figure 5: Position correction using local pressure field. Orthogonal unit vectors $\hat{\vec{f}}$ and $\hat{\vec{g}}$ are in plane perpendicular to vorticity vector. Method of steepest descent is used to locate local pressure minimum.

Figure 6(a).

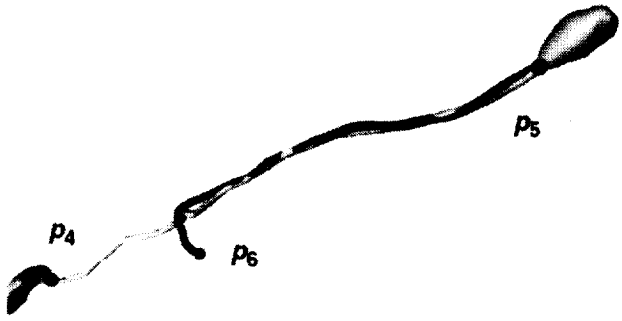

Figure 6(b).

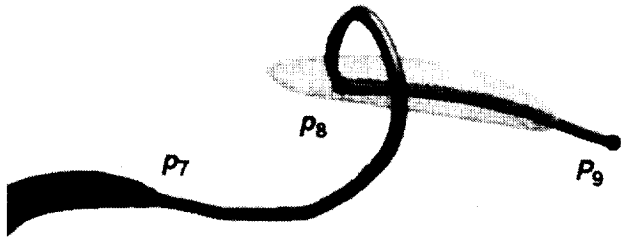

Figure 6(c).

Figure 6: Schematic of line-termination procedure. (a) Forward integration from P_1 to P_2 gives approximately same path as reverse integration from P_2 to P_3, so points P_1 and P_2 are connected by weak vortex. (b) Forward integration from P_4 to P_5 differs markedly from reverse integration from P_5 to P_6, so vortex terminates at P_4. (c) Forward integration from P_7 to P_8 intersects the side of new vortex tube (shown as wireframe). Reverse integration from P_8 to P_9 goes along axis of new vortex away from original tube. Distance from P_7 to P_9 is large, so two vortices are not linked.

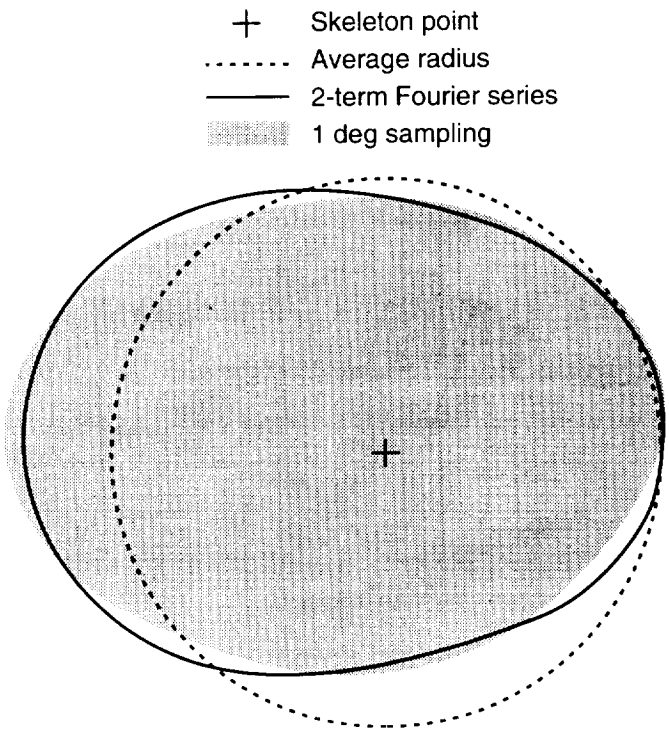

Figure 7: Comparison of different ways to represent vortex cross section. Central cross indicates point on skeleton line. Finely sampled vortex cross section is represented by shaded region. Dashed line is circle with averaged radius. Solid line is two-term Fourier representation of vortex cross section.

Figure 8: Many interacting vortices are educed from direct numerical simulation data with predictor-corrector algorithm.

REPORT DOCUMENTATION PAGE

Form Approved
OMB No. 0704-0188

Public reporting burden for this collection of information is estimated to average 1 hour per response, including the time for reviewing instructions, searching existing data sources, gathering and maintaining the data needed, and completing and reviewing the collection of information. Send comments regarding this burden estimate or any other aspect of this collection of information, including suggestions for reducing this burden, to Washington Headquarters Services, Directorate for Information Operations and Reports, 1215 Jefferson Davis Highway, Suite 1204, Arlington, VA 22202-4302, and to the Office of Management and Budget, Paperwork Reduction Project (0704-0188), Washington, DC 20503.

1. AGENCY USE ONLY *(Leave blank)*	2. REPORT DATE	3. REPORT TYPE AND DATES COVERED
	March 1994	Contractor Report

4. TITLE AND SUBTITLE
A PREDICTOR-CORRECTOR SCHEME FOR VORTEX IDENTIFICATION

5. FUNDING NUMBERS
C NAS1-19480
WU 505-90-52-01

6. AUTHOR(S)
Bart A. Singer
David C. Banks

7. PERFORMING ORGANIZATION NAME(S) AND ADDRESS(ES)
Institute for Computer Applications in Science
and Engineering
Mail Stop 132C, NASA Langley Research Center
Hampton, VA 23681-0001

8. PERFORMING ORGANIZATION REPORT NUMBER
ICASE Report No. 94-11

9. SPONSORING/MONITORING AGENCY NAME(S) AND ADDRESS(ES)
National Aeronautics and Space Administration
Langley Research Center
Hampton, VA 23681-0001

10. SPONSORING/MONITORING AGENCY REPORT NUMBER
NASA CR-194882
ICASE Report No. 94-11

11. SUPPLEMENTARY NOTES
Langley Technical Monitor: Michael F. Card
Final Report
Submitted to Physics of Fluids

12a. DISTRIBUTION/AVAILABILITY STATEMENT
Unclassified–Unlimited

Subject Category 34, 60

12b. DISTRIBUTION CODE

13. ABSTRACT *(Maximum 200 words)*

A new algorithm for identifying and characterizing vortices in complex flows is presented. The scheme uses both the vorticity and pressure fields. A skeleton line along the center of a vortex is produced by a two-step predictor-corrector scheme. The technique uses the vector field to move in the direction of the skeleton line and the scalar field to correct the location in the plane perpendicular to the skeleton line. A general vortex cross section can be concisely defined with five parameters at each point along the skeleton line. The details of the method and examples of its use are discussed.

14. SUBJECT TERMS
turbulence; direct numerical simulation

15. NUMBER OF PAGES
22

16. PRICE CODE
A03

17. SECURITY CLASSIFICATION OF REPORT	18. SECURITY CLASSIFICATION OF THIS PAGE	19. SECURITY CLASSIFICATION OF ABSTRACT	20. LIMITATION OF ABSTRACT
Unclassified	Unclassified		

National Aeronautics and
Space Administration
Langley Research Center
Mail Code 180
Hampton, VA 23681-00001

Official Business
Penalty for Private Use, $300

BULK RATE
POSTAGE & FEES PAID
NASA
Permit No. G-27